Proceedings of the 8th U.S. National Conference on Earthquake Engineering
April 18-22, 2006, San Francisco, California, USA
Paper No. 1717

SEISMIC EVALUATION OF INFILLED REINFORCED CONCRETE FRAMES STRENGTHENED WITH FRPS

B. Binici[1] and G. Ozcebe[2]

ABSTRACT

There is an urgent need to retrofit the deficient mid-rise reinforced concrete frame buildings in Turkey. For this purpose, an efficient FRP retrofit scheme was developed, in which hallow clay brick infill walls are utilized as lateral load resisting elements. The main premise of this practical retrofit scheme is to limit interstory deformations by FRP strengthened infill walls that are integrated to the boundary frame members through FRP anchors. Based on failure modes and measured deformation limits obtained from a large database of experiments, a diagonal compression-strut and tension-tie model is developed. The model is verified with a number of reinforced concrete frame test results with and without upgrades. Furthermore, results of a case study conducted on a typical building frame revealed that strength levels similar to that of a RC shear wall retrofit scheme can be obtained through the FRP retrofit alternative resulting in a displacement ductility of about four.

.

Introduction

Recent earthquakes in Turkey demonstrated the vulnerability of existing structures to large seismic demands that were not accounted in their design. Hence, there is an urgent need of developing reliable and efficient upgrade methods for the large deficient building stock. Motivated by this, different rehabilitation methods (i.e. use of FRPs, addition of shear walls or precast panels) were examined at Middle East Technical University. Among these alternatives, use of fiber reinforced polymers (FRPs) was found to be an effective alternative with rapid retrofit time and providing substantial increases in strength with limited ductility. In order to design and detail FRPs for seismic retrofit of existing structures, analysis and design procedures need to be established so that the developed retrofit alternative can be used in the upgrades of deficient mid-rise buildings. Modeling guidelines of FRP strengthened infill walls are presented in this study for use along with nonlinear static analysis procedures. Furthermore, pushover analysis results for a deficient building retrofitted with two alternatives, namely FRP retrofit and addition of shear walls are presented.

[1]Assistant Professor, Dept. of Civil Engineering, Middle East Technical University, 06531, Ankara, Turkey.
[2]Professor, Dept. of Civil Engineering, Middle East Technical University, 06531, Ankara, Turkey.

Observed Behavior

When a reinforced concrete frame with infill walls is subjected to lateral deformations, the infill wall acts as a diagonal strut, while the separation of the infill occurs on the opposite side. The idea of the FRP retrofit scheme is to reduce inter-story deformation demands by using FRPs to act as tension ties similar to a steel cross-brace configuration. In order to achieve this, diagonal FRPs bonded on the infill wall is tied to the framing members using FRP anchors as shown in Figure 1. In this way, a tension tie contributes to the load carrying capacity in addition to the strength provided by the compression strut formed along the infill diagonal. Special embedded fan type FRP anchors formed by rolling FRP sheets are connected in the corner region in order to achieve efficient use of FRP materials (Figure 1). To eliminate premature debonding of FRP from plaster surface anchor dowels are used along the thickness of the infill wall (Figure 1).

Experiments conducted on FRP strengthened reinforced concrete frames (Erduran 2002, Erdem 2003, Akgüzel 2003) with infill walls revealed that there are two dominant failure modes (Figure 2). First mode initiates with the failure of the FRP anchors in the form of a combined pull-out and slip failure. As soon as the anchors fail, the load carried by the FRP is transferred to the diagonal compression strut and failure of the infill wall occurs due to corner crushing. When three CFRP anchors with a depth of about five times the hole diameter is used per corner on each side of the infill, it has been observed that anchor failure occurs at an effective diagonal FRP strain of about 0.002-0.003. Second failure mode occurs because of FRP debonding from the infill wall surface. After FRP debonding, previously formed horizontal cracks start to open and when the tie action of FRP is lost, sliding shear failure of the infill wall occurs. First failure mode is mainly due to insufficient anchor depth and can be avoided by increasing the depth and number of anchor dowels. However, the second failure mode marks the limiting strength of the strengthened infill. Tests have shown that beyond a strain level of about 0.006, FRP debonding took place resulting in a sliding shear failure of the infill followed by a sudden drop of strength. These observations obtained from the finite element analysis and experiments are used to develop structural models for the FRP strengthened RC frames with infill walls.

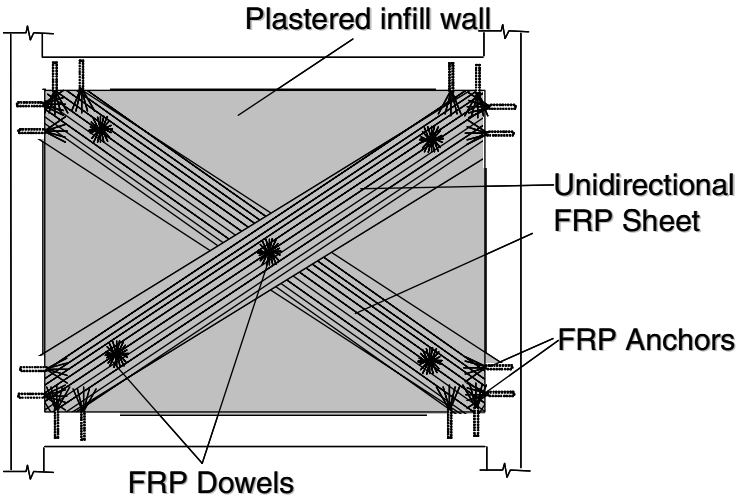

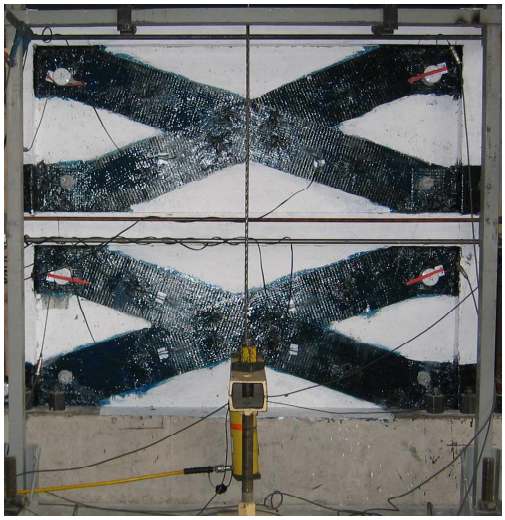

Figure 1. FRP strengthening method for reinforced concrete frames with infill walls

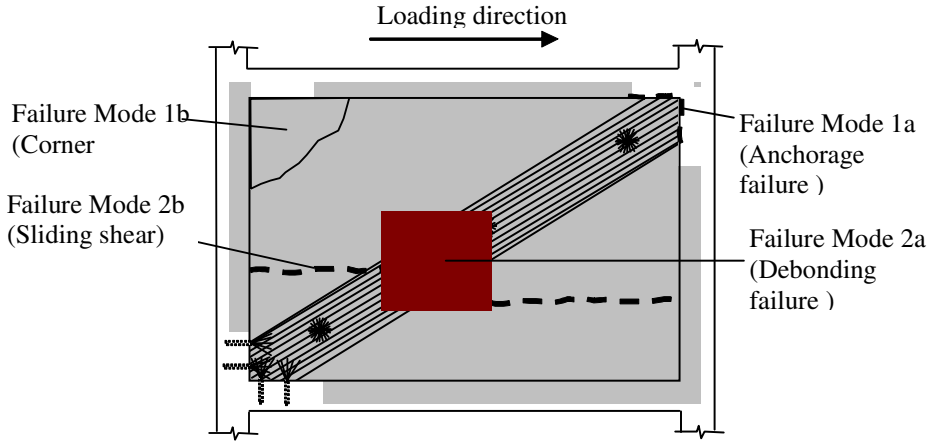

Figure 2. Failure modes of FRP strengthened infill wall in a reinforced concrete frame

Analytical Model

The analytical model of a strengthened frame proposed in this study is a structural one and is shown in Figure 3. Frame elements (beams and columns) are modeled using elastic elements with predefined plastic hinge regions at their ends. The cross sections of the plastic hinge regions are discretized into a number of fibers with appropriate uniaxial stress-strain behavior for different materials. Unconfined concrete fibers are modeled using Hognestad stress-strain curve with a linear descending branch up to a strain of 0.004 at zero stress. Modified Kent and Park model is implemented for core concrete fibers confined with transverse reinforcement. Steel reinforcement is modeled with an elastic perfectly plastic material model. The advantage of fiber models is the consideration of axial load moment interaction during analysis and avoiding the need of performing sectional analysis separately. Plastic hinge length, which is the length of the region where inelastic action is expected, is taken equal to the depth of the member. Effective cracked stiffness equal to the 75% of the gross section properties and modulus of elasticity of concrete are used between the plastic hinge regions to model the elastic portion of the frame elements.

FRP Ties

Infill wall strengthened using FRPs is modeled using a compression strut and a tension tie (Figure 3), which adequately represents the load transfer mechanism observed from the experiments and finite element analysis. A trilinear stress-strain response is proposed for the truss members to simulate the behavior of the strengthened infill wall (Figure 3). Experiments conducted on reinforced concrete frames with infill walls with and without plaster showed that presence of plaster on infill wall surface needs to taken into account for accurate estimation of stiffness and strength. Therefore it assumed here that FRP, infill material and plaster on the infill wall surface contributes to the stiffness of the tension tie. The area of the composite tension tie is:

$$A_{tie} = w_f t_{tie} \tag{1}$$

where w_f is the width of the FRP provided and t_{tie} is given by:

$$t_{tie} = t_f + t_p + t_{in} \tag{2}$$

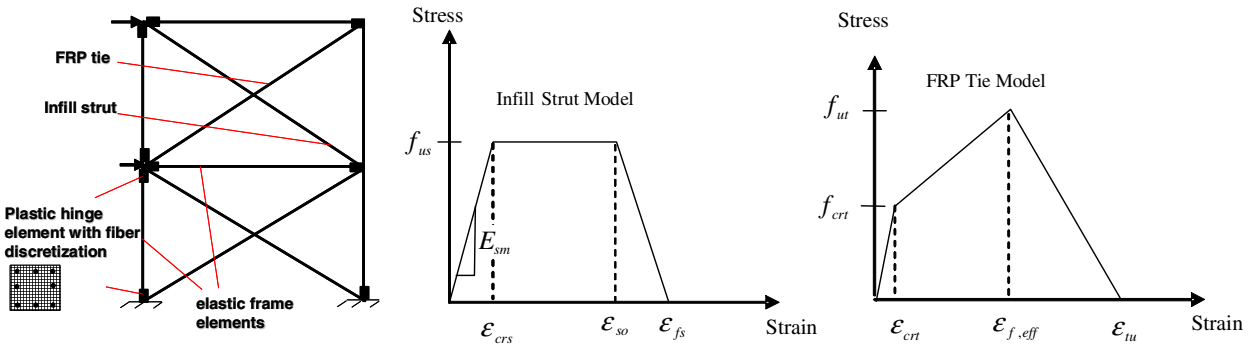

Figure 3. Structural Modeling and Stress-Strain Models for Infill Struts and FRP Ties

in which t_f, t_p, t_{in} are the thicknesses of FRP, infill and plaster, respectively. It is not unrealistic to assume that mortar used between the infill blocks is similar to the plaster used for exterior coating. Therefore cracking stress of the tie, f_{crt} can be found from:

$$f_{crt} = \frac{V_{crt}}{A_{tie}} \tag{3}$$

$$V_{crt} = f_{pt} w_f \left(\left(t_{in} + t_p \right) + \frac{E_f}{E_m} t_f \right) \tag{4}$$

where f_{pt} is the tensile strength of the plaster, E_f and E_m are the moduli of elasticity of FRP and mortar, respectively. Eq. (4) assumes that cracking of plaster and mortar occurs simultaneously up to which the three-phase material behaves as a unit. The corresponding cracking strain, ε_{crt} is the cracking strain of the plaster which can be determined from uniaxial tension tests. Beyond cracking, contribution of mortar and plaster to load carrying capacity gradually decreases (Figure 3). Tensile capacity V_{ut}, and tensile strength, f_{ut}, can be computed from Eqs. (5) and (6) respectively, based on the capacity of the FRP at the effective strain obtained from experimental results, $\varepsilon_{f,eff}$, at which anchor failure or debonding initiates.

$$V_{ut} = \varepsilon_{f,eff} w_f t_f E_f \tag{5}$$

$$f_{ut} = \frac{V_{ut}}{A_{tie}} \tag{6}$$

Last definition required for the tension tie is the strain at which complete failure of FRP occurs (ε_{tu}). This strain limit controls descending portion of the global response. The preliminary analyses results showed that three times the effective strain ($\varepsilon_{f,eff}$) can be used to model the strength degradation beyond ultimate strength.

Infill Struts

The strut stress-strain model is also a trilinear model with a perfectly plastic plateau and limited deformation capacity. The area of the composite strut, A_{str}, is computed by:

$$A_{st} = w_s t_{st} \tag{7}$$

where

$$t_{st} = t_p + t_{in} \tag{8}$$

$$w_s = \frac{(1-\alpha)\alpha h}{\cos\theta} \tag{9}$$

Eq. (9) is proposed by El-Dakhakhi et. al. (2003) based on the work by Saneinejad and Hobbs (1995) to estimate the effective width of the strut. In Eq. (9), h is the height of the infill wall, θ is the strut inclination angle and α is a dimensionless parameter to account for the frame infill contact length computed by:

$$\alpha = \sqrt{\frac{2(M_{pj} + 0.2M_{pc})}{h^2 t_{st} f_{mc}}} \tag{10}$$

in which M_{pj} is the minimum of the moment capacities of the column or the beam, M_{pc} is the moment capacity of the column and f_{mc} is the compressive strength of the infill plaster composite.

The ultimate strength of the diagonal compressive strut V_{us}, is computed based on the minimum of the two capacities, namely sliding shear, V_{ss}, and corner crushing, V_{cc}.

$$V_{us} = \min(V_{ss}, V_{cc}) \tag{11}$$

$$V_{ss} = f_{mv} L t_{st} \tag{12}$$

$$V_{cc} = 250 t_{st} f_{mc} \tag{13}$$

and the ultimate strength, f_{us}, can be computed by:

$$f_{us} = \frac{V_{us}}{A_{st}} \tag{14}$$

In Eq. (12), f_{mv} is the shear strength of the mortar (or plaster) bed joint and *L* is the width of the infill wall. Eq. (13) is an empirical equation calibrated with test results and proposed by Flanagan and Bennett (1999) to predict corner crushing strength of infill walls. f_{mc} that appears in Eqs. (10) and (13) and the slope of the stress strain curve in Figure 3 (E_{sm}), can be obtained from uniaxial compression tests of plastered infill walls. In the absence these tests Eqs. (15) and (16) can be used to predict the strength and stiffness of the diagonal strut.

$$f_{mc} = \frac{f_{in} t_{in} + f_m t_p}{t_{st}} \tag{15}$$

$$E_{sm} = \frac{E_{in} t_{in} + E_m t_p}{t_{st}} \tag{16}$$

In Eq. (16), E_{in} is the elasticity modulus of the infill material, which generally varies between 500 to 1500 times the compressive strength of the infill material. Strain value at which strength loss initiates has been observed to occur after the failure of FRP tie. Therefore, ε_{so} should be larger than $\varepsilon_{f,eff}$ in the presence of FRPs and should be equal to the cracking strain of mortar (ε_{crs}) in the absence of any strengthening. Following relationship proved to yield satisfactory estimations for the deformation capacity of the strut:

$$\varepsilon_{so} = \begin{cases} \varepsilon_{crs} \text{ without FRP} \\ 2\varepsilon_{f,eff} \text{ with FRP} \end{cases} \tag{17}$$

Eq. (17) implies that no ductility should be expected for the compression strut in the absence of FRP strengthening whereas some ductility is available for the strut when FRPs are used delaying the complete failure. Failure strain of the compression strut, ε_{fs}, was assumed to occur at a strain of 0.01 by El-Dakhakhni et. al. (2003). A similar assumption is made here for the infill walls without any strengthening or failing due to anchorage failure. This strain limit can be taken as 0.02 when failure of the FRP tie occurs beyond a strain level of 0.005.

Experimental Verification

Akgüzel (2003) tested four two-story one bay frames, two of them unstrengthened and two with FRP upgrades. All the columns in the frame members were deficient for confining steel and had lap splices in the plastic hinge regions. Details of material properties and test specimens are given in Tables 1 and 2, respectively. Lateral load was applied incrementally and lateral load ratio of the second story to the first story was two throughout the tests. One of the unstrengthened specimens had no infill walls whereas the other one had infill walls in both stories. Strengthening was achieved through bonding of 200 mm wide FRP sheets on both sides of the frame. Total base shear plotted against roof displacement values are compared for the analytical and experimental results in Figure 4. FRP strain limit was taken as 0.006 for the case when FRP debonding was the failure mode and 0.002 was used when anchor strength was critical. It can be observed that FRP strengthening resulted in an increase of about 100% in base shear capacity when proper anchors were used. Estimations of stiffness and strength of all the test specimens reasonably agree with the measured response.

Erdem (2003) tested two three-bay two-story frames, one bare frame and one infilled frame strengthened with FRPs. Load was applied to the second story floor level only. Strengthened specimen had infills only in the center bay of the frame. Confining steel deficiencies and lap splices in the plastic hinge region existed in these specimens. Strengthening was performed by bonding 400 and 200 mm wide FRPs on the infills of the first and second story infill walls, respectively. Details of material properties and test specimens are given in Tables 1 and 2, respectively. Analyses results are shown together with experimental results for total base shear versus roof displacement in Figure 5. A strain limit of 0.002 was used to curves obtained from these tests are compared herein with the pushover tests using the models described above.

It can be observed that capacity of the strengthened frame is approximately twice that of the one prior to upgrading. Furthermore, behavior of the strengthened frame approaches the behavior of the bare frame at large lateral deformations. Analytical estimations of ultimate strength and corresponding deformations agree well with the measured values.

Table 1. Details of experiments

Researcher	Material	Compressive Strength (MPa)	Tensile Strength (MPa)	Modulus of Elasticity (Mpa)
Erdem (2003)	FRP	-	3450	230000
	Concrete	9.5	-	14600
	Plaster	5	0.5	9800
	Infill	11.2 (2)	-	7000 (2000) [1]
Akgüzel (2003)	FRP	-	3450	230000
	Concrete	15	-	18400
	Plaster	5	0.5	10600
	Infill	11 (2)	-	7000 (2000)

1) Numbers in parenthesis denote values in the weak direction of infill material.

Table 2. Member details for analyzed frames

Researcher	Columns				Beams			Anchors	
	Dimensions (mm x mm)	ρ_l [1] (%)	s [2] (mm)	l_d [3] (mm)	Dimensions (mm x mm)	ρ_l (%)	s (mm)	n [4]	d [5] (mm)
Erdem (2003)	110 x 110	1.6	100	320	110 x 150	1.4	100	3	70
Akgüzel (2003)	100 x 150	1.3	95	160	150 x 150	1.3	130	3 (5) [6]	50 (80)

1) Longitudinal reinforcement ratio ; 2) Spacing of transverse reinforcement ; 3) Lap splice length in the plastic hinge region

4) Depth of anchors ; 5) Number of anchors ; 6) Values for specimen failed with FRP debonding

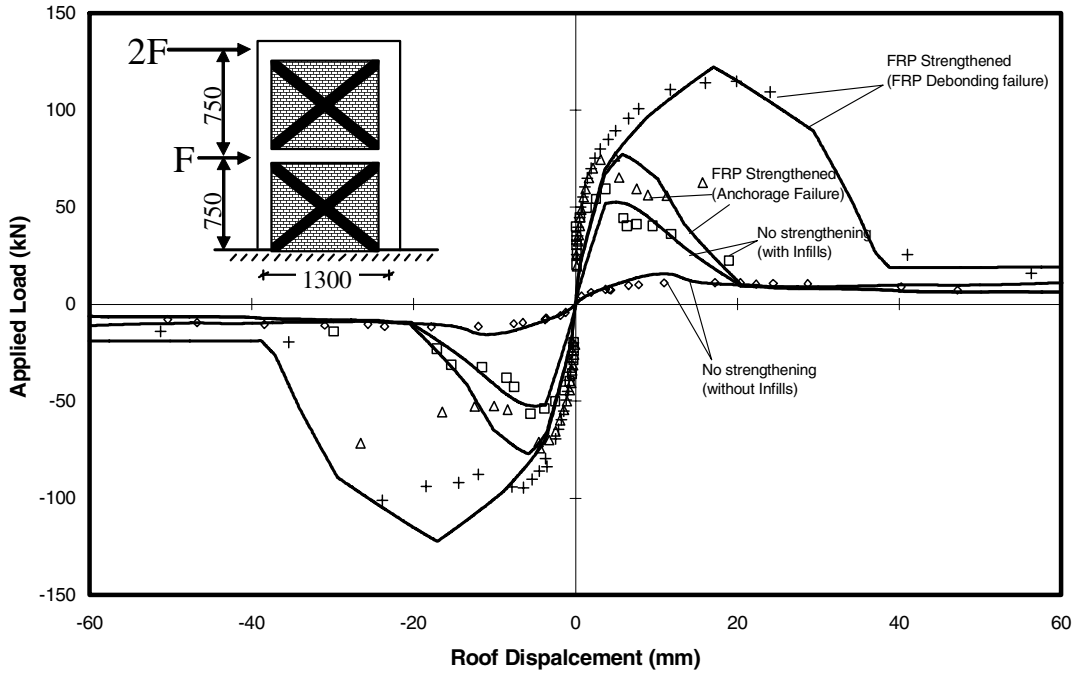

Figure 4. Comparisons of experiments conducted by Akguzel (2003) with analysis results (Points are the experimental points, lines are analytical estimations)

Case Study

A typical interior frame of a regular plan building requiring upgrade was analyzed to demonstrate the capacity increases that can be obtained through the use of FRPs. The elevation view of the four-bay, five-story building frame including the locations of the infill walls is shown in Figure 6. All the columns were 400 mm x 400 mm with a longitudinal reinforcement ratio of 1% whereas the beams had dimensions of 300 mm x 600 mm with 0.5% longitudinal reinforcement ratio. Stirrup spacing of the columns were approximately equal to the effective depth of the section resulting in insufficient confinement for ductile behavior. Concrete strength was 10 MPa simulating typical construction quality in Turkey whereas the reinforcement had a yield strength of 420 MPa. The infill walls were composed of hollow-clay brick with a thickness of 100 mm and a compressive strength of 2 MPa. Additional plaster on the infill walls was 40 mm thick with a compressive strength of about 2 MPa.

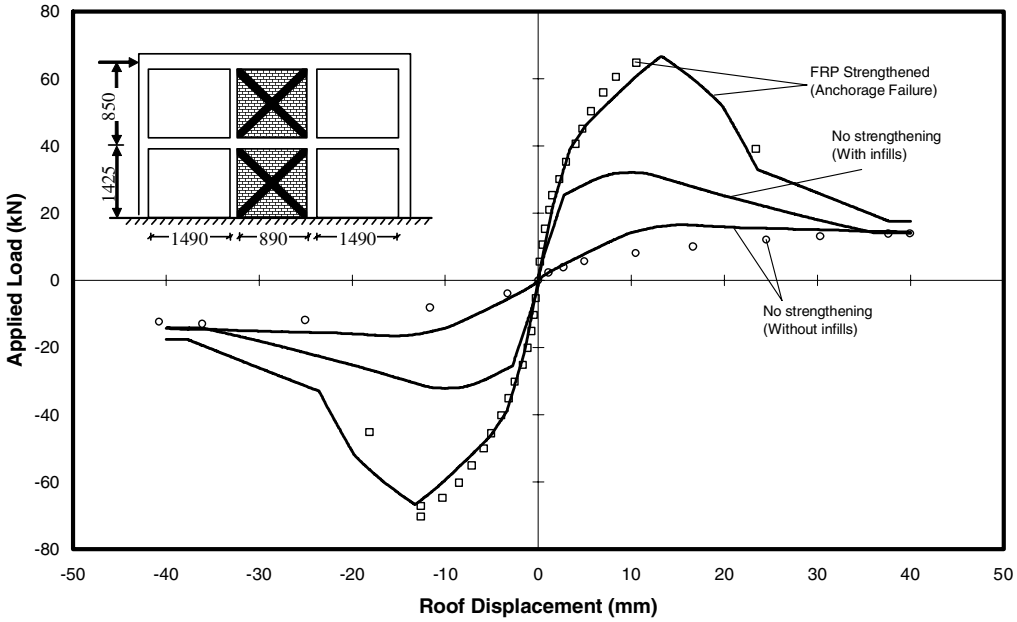

Figure 5. Comparisons of Experiments conducted by Erdem (2003) with analysis results (Points are the experimental points, lines are analytical estimations)

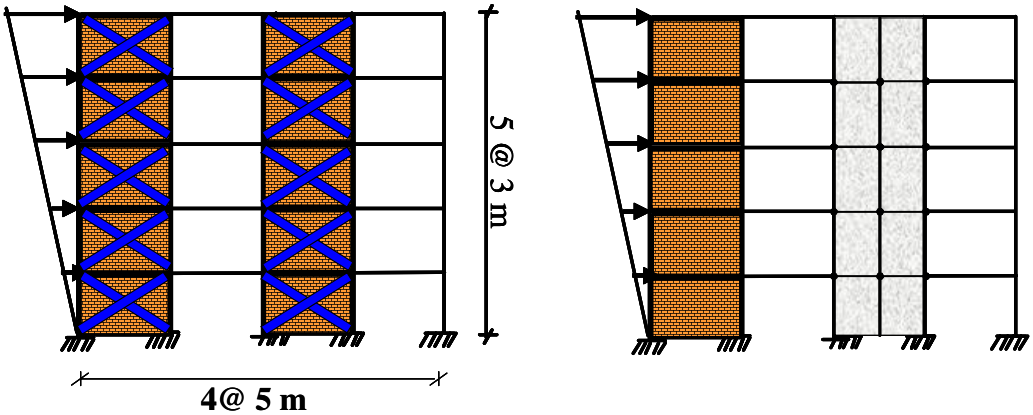

(a) FRP Strengthening (b) Addition of Shear-wall

Figure 6. Applied Retrofit Alternatives

Two retrofit alternatives were designed as shown in Figure 6. First retrofit employed carbon fiber reinforced polymers with material properties given in Table 1. Retrofit design was conducted by considering a CFRP width similar to the width of the estimated compression strut (750 mm). In this way, the compression struts can remain intact and sustain large deformations prior to failure of FRP ties. Sufficient CFRP anchors were provided to eliminate anchorage failures. Second alternative was a conventional shear wall addition that is commonly employed in Turkey. The brick infill walls in the third bay of the frame were completely removed and a shear wall having 200 mm thickness, 0.3% longitudinal reinforcement ratio with a concrete compressive strength of 40 MPa was constructed.

Four cases were analyzed by subjecting the frames to an inverted triangular displacement profile along the building height (Figure 6). First analysis was conducted by neglecting the presence of the infill walls. Second analysis was performed by considering the presence of infill walls as strut elements. A third analysis was conducted by performing an upgrade of the building with CFRPs. All the infill walls were modeled using compression struts and FRP ties as described in detail in previous sections. The final analysis was conducted for the shear-wall added case, in which walls were modeled using beam column elements along the centerline of the wall. The connection between the wall and neighboring frame elements were provided through rigid links. Normalized base shear ratio was plotted against the normalized roof displacement in Figure 7 to compare the response of different scenarios. It can be observed that presence of the infill walls increases the lateral load carrying capacity by about 30%, whereas the displacement capacity of the building decreases due to rapid degradation of the infill walls and neighboring frame elements once the base shear capacity is reached. Analysis results show that CFRP retrofit resulted in strength increases of about 90% compared to the bare frame whereas capacity increase was about 50% prior to strengthening with infill walls. It can also be observed that at large displacements, lateral load carrying capacity approaches to that of the bare frame. On the other hand RC-wall retrofit resulted in similar lateral strength levels as the FRP retrofit alternative. Ductility of the RC-wall alternative was found to result in a ductile behavior whereas the FRP retrofit yields limited ductility mainly due to progressive failure of the strengthened infill walls. As a result it is possible to say that application of the CFRP retrofit can enhance both the load carrying capacity and deformation capacity of reinforced concrete frames with infill walls. Furthermore, it was interesting to observe that to achieve lateral load carrying capacity similar to shear wall retrofitted case, infill wall area approximately twice the shear wall area had to be strengthened using FRPs.

Conclusions

A strut and tie approach proposed in this study to model FRP strengthened infill walls was proved to result in accurate estimations of strength and inelastic deformation capacity of tested frames. The case study conducted on a deficient frame showed that with the FRP retrofit scheme it is possible to achieve strength levels similar to those that can be obtained by addition of shear walls. Although not as ductile as the frame with a shear wall, the FRP retrofitted frame had a displacement ductility of about four. It can be concluded that in the presence of sufficient area of infill walls that can be strengthened with FRPs this retrofit alternative can provide rapid retrofits removing the need to relocate the occupants. In this way, it can be possible to retrofit regions with thousands of buildings within months.

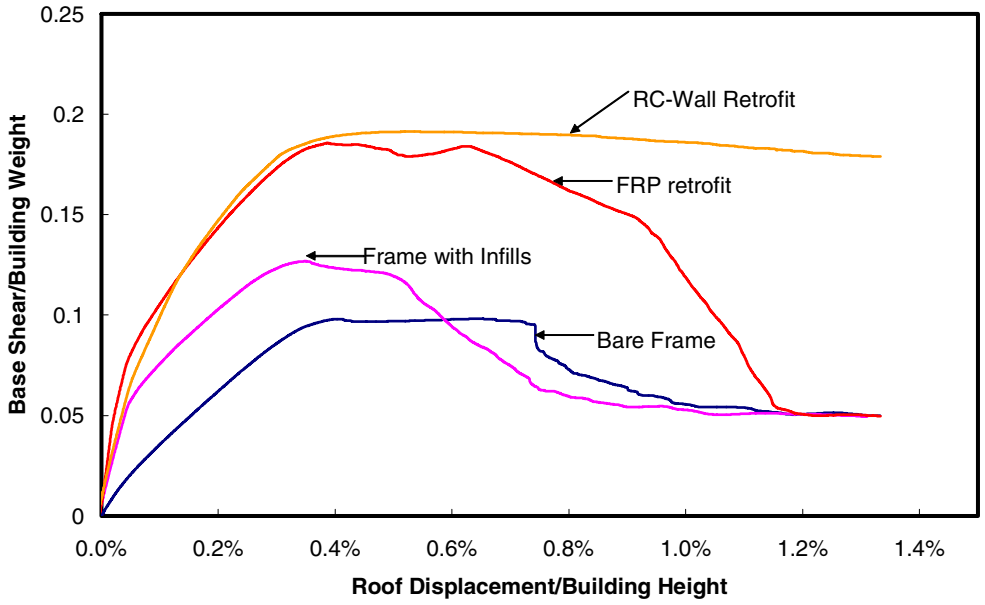

Figure 7. Analysis results for the building frame analysis for different cases

References

Erduran, E., 2002. Behavior of brick infilled reinforced concrete frames strengthened by CFRP reinforcement: Phase 2, MS thesis submitted to Middle East Technical University, Department of Civil Engineering, p. 77.

Erdem, I., 2003. Strengthening of existing reinforced concrete frames, MS thesis submitted to Middle East Technical University, Department of Civil Engineering, p. 123.

Akguzel, U., 2003. Seismic retrofit of brick infilled R/C frames with lap splice problem in columns, MS thesis submitted to Bogazici University, Department of Civil Engineering, p. 125

El-Dakhakhni, W., Elgaaly, M., and Hamid, A., 2003. Three-strut model for concrete masonry infilled steel frames, *ASCE, Journal of Structural Engineering*, 129(2), 177-185.

Saneinejad, A., and Hobbs, B., 1995. Inelastic design of infilled frames, *ASCE, Journal of Structural Engineering*, 121(4), 634-650.

Flanagan, R.D., and Bennett, 1999. In-plane behavior of structural clay tile infilled frames, *ASCE, Journal of Structural Engineering*, 125(6) 590-599.